

Absence of magnetic order for the spin-half Heisenberg antiferromagnet on the star lattice

J. Richter,¹ J. Schulenburg,² A. Honecker,³ and D. Schmalfuß¹

¹*Institut für Theoretische Physik, Universität Magdeburg, P.O. Box 4120, D-39016 Magdeburg, Germany*

²*Universitätsrechenzentrum, Universität Magdeburg, P.O. Box 4120, D-39016 Magdeburg, Germany*

³*Institut für Theoretische Physik, TU Braunschweig, D-38106 Braunschweig, Germany*

(Dated: June 2, 2004; revised September 13, 2004)

We study the ground-state properties of the spin-half Heisenberg antiferromagnet on the two-dimensional star lattice by spin-wave theory, exact diagonalization and a variational mean-field approach. We find evidence that the star lattice is (besides the kagomé lattice) a second candidate among the 11 uniform Archimedean lattices where quantum fluctuations in combination with frustration lead to a quantum paramagnetic ground state. Although the classical ground state of the Heisenberg antiferromagnet on the star lattice exhibits a huge non-trivial degeneracy like on the kagomé lattice, its quantum ground state is most likely dimerized with a gap to all excitations. Finally, we find several candidates for plateaux in the magnetization curve as well as a macroscopic magnetization jump to saturation due to independent localized magnon states.

PACS numbers: 75.10.Jm; 75.45.+j; 75.60.Ej; 75.50.Ee

I. INTRODUCTION

The spin-half two-dimensional (2D) Heisenberg antiferromagnet (HAFM) has attracted much attention in recent times. In particular, the recent progress in synthesizing novel quasi-2D magnetic materials exhibiting exciting quantum effects has stimulated much theoretical work. We mention for example the spin-gap behavior in CaV_4O_9 ¹ and in $\text{SrCu}_2(\text{BO}_3)_2$,² the spin fractionalization in Cs_2CuCl_4 ³ or the plateau structure in the magnetization process of frustrated quasi-2D magnetic materials like $\text{SrCu}_2(\text{BO}_3)_2$ ² or Cs_2CuBr_4 .⁴

While the ground state (GS) of the one-dimensional quantum HAFM does not possess Néel long-range order, for the spin-half HAFM on 2D lattices the competition between quantum fluctuations and interactions seems to be well balanced and magnetically ordered and disordered GS phases may appear. A fine tuning of this competition may lead to zero temperature transitions between semi-classical and quantum phases. The prototypes of 2D arrangements of spins are the 11 uniform Archimedean lattices (tilings), see, e.g. Refs. 5,6,7. They present an ideal possibility for a systematic study of the interplay of lattice geometry and magnetic interactions in 2D quantum spin systems.

The HAFM on the widely known square, honeycomb, triangular and kagomé lattices has been studied in numerous papers over the last decade. While for the square, honeycomb and triangular lattices the existence of semi-classical magnetic order seems to be well-established (see e.g. Refs. 7,8,9) the spin-half HAFM on the kagomé lattice is a candidate for a magnetic system with a quantum paramagnetic GS (see the reviews 7,8,9,10 and references therein). Other less known Archimedean lattices like the maple-leaf lattice,¹¹ the square-hexagonal-dodecagonal lattice^{12,13} and the trellis lattice^{14,15} exhibit most likely semi-classical magnetic GS order.

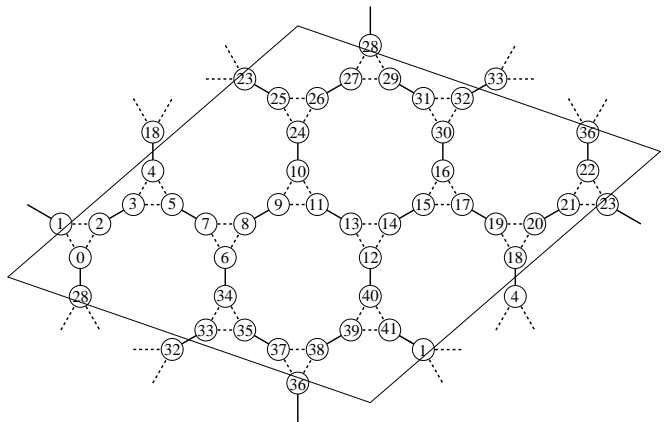


FIG. 1: The star lattice with $N = 42$ sites.

In this paper we present another candidate for a quantum paramagnetic GS among the Archimedean lattices, namely the so-called star lattice, featured by low coordination number $z = 3$ and strong frustration due to a triangular arrangement of bonds (see Fig. 1).

II. MODEL

The geometric unit cell of the star lattice contains six sites and the underlying Bravais lattice is a triangular one (see Figs. 1 and 2). For this lattice we consider the spin-half HAFM in a magnetic field h

$$\hat{H} = J \sum_{\langle ij \rangle} \mathbf{S}_i \cdot \mathbf{S}_j - h \hat{S}^z, \quad (1)$$

where the sum runs over pairs of neighboring sites $\langle ij \rangle$ and $\hat{S}^z = \sum_i \hat{S}_i^z$. The star lattice carries topologically inequivalent nearest-neighbor (NN) bonds J_D (dimer bonds, solid lines in Fig. 1) and J_T (triangular bonds,

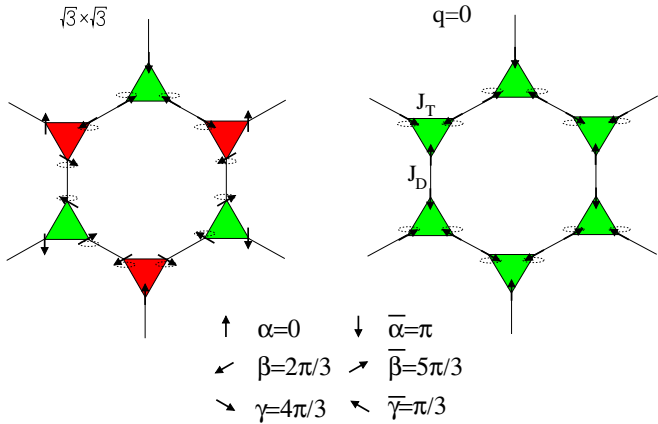


FIG. 2: (Color online) Two variants of the GS of the classical HAFM on the star lattice: the $\sqrt{3} \times \sqrt{3}$ state (left) and the $q=0$ state (right). The dotted ellipses show further degrees of freedom of the highly degenerate classical GS. Different shades of the triangles symbolize different chiralities.

dashed lines in Fig. 1, see also Fig. 2). For the uniform lattice these bonds are of equal strength $J_D = J_T = J$.

III. SEMI-CLASSICAL GROUND STATE

In the classical GS for $h = 0$ the two non-equivalent NN bonds of the star lattice carry different NN spin correlations: The angle between neighboring spins on dimer bonds J_D is π , whereas the angle on triangular bonds J_T is $2\pi/3$. Its energy per bond is $e_0^{\text{class}} = -1/6$. The classical GS for the star lattice has a great similarity to that of the kagomé lattice. It also exhibits a non-trivial infinite degeneracy. Moreover, there are also the two variants of the classical GS, namely the so-called $\sqrt{3} \times \sqrt{3}$ and $q = 0$ states (see Fig. 2), often used for discussing possible order in the kagomé lattice. Hence these two particular planar states can also be considered as variants of possible GS ordering for the star lattice. In the following we discuss the influence of quantum fluctuations on the GS properties.

First, we perform a linear spin-wave theory (LSWT) starting from the planar classical GSs. The LSWT for the star lattice is more ambitious than for the kagomé lattice, since we have to consider six types of magnons. As in the kagomé case^{16,17,18} the spin-wave spectra are equivalent for all coplanar configurations satisfying the classical GS constraint. We obtain six spin-wave branches. Two dispersionless modes are found, namely $\omega_{1\mathbf{q}} = 0, \omega_{2\mathbf{q}} = Js\sqrt{3}$. Thus also a flat zero-mode appears as it is observed for the kagomé case. In addition there are two acoustical and two optical branches. There is no *order-by-disorder* selection among the coplanar classical GSs due to the equivalence of the spin-wave branches obtained from LSWT, exactly like for the kagomé lattice.^{10,17} The GS energy per bond for $s = 1/2$ in LSWT is $e_0/J = -0.296759$. Due to the flat zero mode the in-

tegral for the sublattice magnetization diverges¹⁸ which might be understood as another hint for the absence of the classical order. Although on the semi-classical LSWT level both the kagomé and the star lattice exhibit almost identical properties, the situation might be changed taking into account the quantum fluctuations more properly.

IV. LANCZOS EXACT DIAGONALIZATION

We consider now the extreme quantum limit $s = 1/2$ by direct numerical calculation of the GS and the low-lying excitations at $h = 0$ for finite lattices of $N = 18, 24, 30, 36, 42$ sites. For each size N we have chosen only lattices having good geometric properties using the criteria given in Ref. 19. The largest lattice ($N = 42$) is shown in Fig. 1 and required a Lanczos diagonalization in dimension 801 258 898 for the computation of GS properties. The GS for all these lattices is a singlet and has an energy per bond $e_0 = -0.312479$ ($N = 18$); -0.311342 (24); -0.310808 (30); -0.310348 ($36A$); -0.310657 ($36B$); -0.309918 (42). The first excitation is a triplet and has a gap $\Delta = 0.578710$ ($N = 18$); 0.531822 (24); 0.498564 (30); 0.480343 ($36A$); 0.483112 ($36B$) (no result available for $N = 42$).

We present in Table I the spin-spin correlation for the largest finite lattice considered. Note that the two non-equivalent NN correlation functions differ drastically, we have $\langle \hat{S}_0^z \hat{S}_{28}^z \rangle \sim 3.5 \langle \hat{S}_0^z \hat{S}_1^z \rangle$ indicating a tendency to form local singlets on the dimer bonds.

Let us compare the spin correlations with those for the HAFM on triangular and kagomé lattices. We consider the strongest correlations as a measure for magnetic order and present in Fig. 3 the maximal absolute correlations $|\langle \hat{S}_0^z \hat{S}_i^z \rangle|_{\text{max}}$ for a certain separation $R = |\mathbf{R}_0 - \mathbf{R}_i|$ versus R . As expected we have very rapidly decaying correlations for the disordered kagomé case, whereas the correlations for the Néel ordered triangular lattice are much stronger for larger distances and show a kind of saturation for larger R . Although the correlations for the star lattice are slightly larger than those of the kagomé lattice they are significantly weaker for separations $R \geq 3$ than

TABLE I: All non-equivalent GS spin-spin correlations $\langle \hat{S}_0^z \hat{S}_i^z \rangle = \frac{1}{3} \langle \mathbf{S}_0 \mathbf{S}_i \rangle$ for the HAFM on the star lattice with $N = 42$ sites. In addition to the site index i we give the separation $R = |\mathbf{R}_0 - \mathbf{R}_i|$ between sites 0 and i in units of NN separation.

i (R)	1 (1)	3 (1.932)	4 (2.909)
$\langle \hat{S}_0^z \hat{S}_i^z \rangle$	-0.05643	0.03559	-0.01058
i (R)	6 (3.732)	7 (3.346)	9 (5.278)
$\langle \hat{S}_0^z \hat{S}_i^z \rangle$	-0.00451	0.01066	0.00439
i (R)	10 (4.625)	26 (2.732)	28 (1)
$\langle \hat{S}_0^z \hat{S}_i^z \rangle$	-0.01173	-0.03875	-0.19707

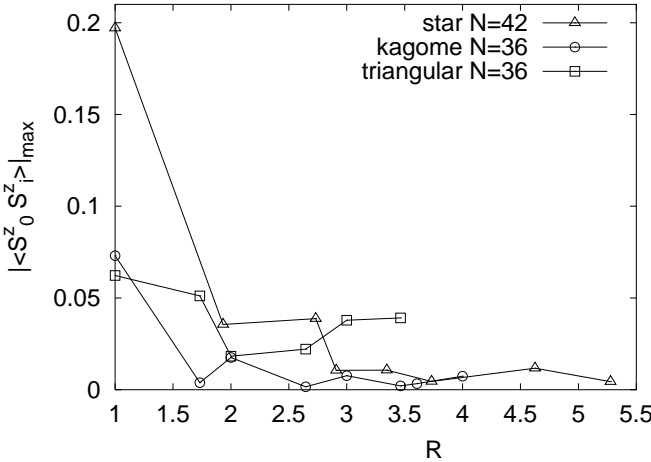


FIG. 3: Maximal spin-spin correlation $|\langle \hat{S}_0^z \hat{S}_i^z \rangle|_{\max}$ versus separation $R = |\mathbf{R}_0 - \mathbf{R}_i|$ for the star lattice ($N = 42$), the kagomé ($N = 36$) and the triangular lattice ($N = 36$) (the lines are guides for the eyes). The data for the kagomé lattice coincide with those from Ref. 20.

those of the triangular lattice. The large NN correlation for the star lattice corresponds to a NN dimer bond.

Next we consider the low-lying spectrum of the star lattice (see Fig. 4), following the lines of the discussion of the spectrum for the triangular²¹ and the kagomé lattice.^{22,23} It is obvious that the lowest states $E_{\min}(S)$ are not well described by the effective low-energy Hamiltonian $H_{\text{eff}} \sim E_0 + \mathbf{S}^2/2N\chi_0$ of a semi-classically ordered system: (i) The E_{\min} versus $S(S+1)$ curve deviates significantly from a straight line (cf. the dashed line in Fig. 4). (ii) We do not see well separated lowest states in the different sectors of S (so-called quasi degenerate joint states²¹) which could collapse onto a Néel-like state in the thermodynamic limit. (iii) The symmetries of the lowest states in each sector of S cannot be attributed to the classical $\sqrt{3} \times \sqrt{3}$ or $q=0$ GSs in general. These features are similar to the kagomé lattice.^{22,23} However, there is one striking difference. In contrast to the kagomé lattice we do not have non-magnetic singlets filling the singlet-triplet gap (spin gap) commonly interpreted as a remnant of the huge classical GS degeneracy. Rather we have a particularly large singlet-singlet gap. This basic difference to the kagomé lattice can be attributed to the special property of the quantum GS of the star lattice to have strongly enhanced antiferromagnetic correlations on the J_D bonds. As a consequence the quantum GS of the star lattice has an exceptionally low GS energy e_0 (see Table II) and is well separated from all excitations.

For finite systems the order parameter is based on the spin-spin correlation functions. For systems with well-defined semi-classical long-range order usually the square of the staggered magnetization is used. However, this definition of the order parameter is problematic in the present situation: due to the huge non-trivial degeneracy of the classical GS it remains unclear which type of ordering might be favored in the quantum system. Therefore

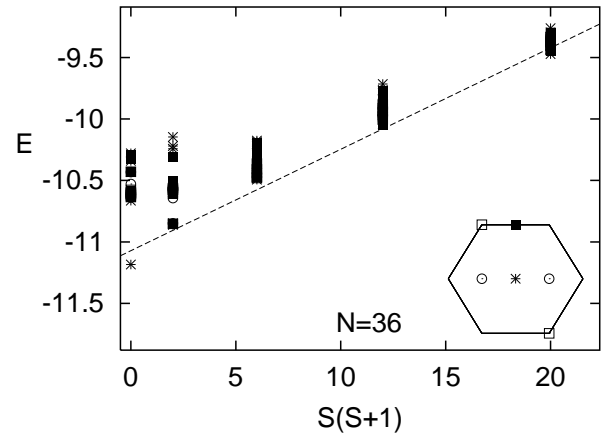


FIG. 4: Low-energy spectrum for the HAFM on the star lattice ($N = 36B$) (the inset shows the \mathbf{k} points in the Brillouin zone).

we use a definition of an order parameter

$$m^+ = \left(\frac{1}{N^2} \sum_{i,j} |\langle \mathbf{S}_i \mathbf{S}_j \rangle| \right)^{1/2} \quad (2)$$

which is independent of any assumption on classical order.⁷ For bipartite systems like the square lattice this definition is identical to the staggered magnetization \bar{m} and for the HAFM on the triangular lattice $(m^+)^2$ is by 1/3 larger than the usual definition.⁷ For the two planar classical $\sqrt{3} \times \sqrt{3}$ and $q=0$ GSs we get $m_{\text{class}, \sqrt{3} \times \sqrt{3}}^+ = m_{\text{class}, q=0}^+ = \frac{1}{2} \sqrt{2/3} \approx 0.40825$ (note that for the kagomé lattice one obtains the same value). For the quantum model one finds $(m^+)^2 = 0.149113$ ($N = 18$); 0.114822 (24); 0.094831 (30); 0.082299 ($36A$); 0.079351 ($36B$); 0.073251 (42). For comparison we quote the values for the $N = 36$ kagomé lattice: $(m^+)^2 = 0.059128$, and the $N = 36$ triangular lattice: $(m^+)^2 = 0.124802$.

We have performed finite-size extrapolations based on the standard formulas for 2D spin-half Heisenberg anti-ferromagnets (see, e.g. Refs. 7,24,25), namely $e_0(L) = A_0 + \frac{A_3}{L^3} + \mathcal{O}(L^{-4})$ for the GS energy per bond, $m^+(L) = B_0 + \frac{B_1}{L} + \mathcal{O}(L^{-2})$ for the order parameter, and $\Delta(L) = G_0 + \frac{G_2}{L^2} + \mathcal{O}(L^{-3})$ for the spin gap, where $A_0 = e_0(\infty)$,

TABLE II: Results of the finite-size extrapolation of the GS energy per bond e_0 and the order parameter m^+ (eq. (2)) of the spin-half HAFM for the star ($N = 18, 24, 30, 36, 42$), the kagomé ($N = 12, 18, 24, 30, 36$) and the triangular ($N = 24, 30, 36$) lattices. To see the effect of quantum fluctuations we scale m^+ by its corresponding classical value m_{class}^+ .

lattice	triangular	kagomé	star
e_0	-0.1842	-0.2172	-0.3091
m^+ / m_{class}^+	0.386	0.000	0.122

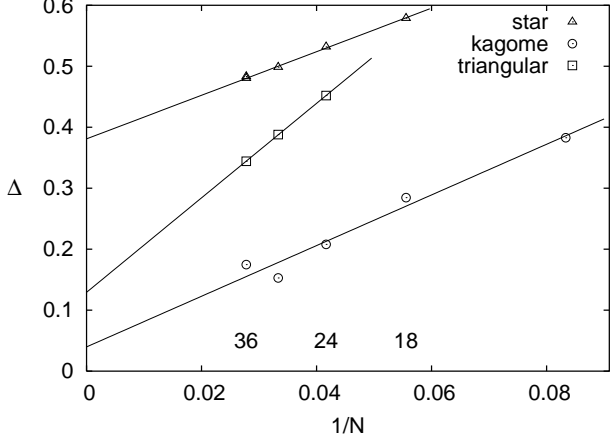


FIG. 5: Finite-size behavior of the spin gap Δ , i.e. the gap to $s = 1$ excitations versus inverse system size $1/N$. Results are shown for the star lattice (triangles) in comparison with those for the kagomé lattice (circles, compare Ref. 23) and the triangular lattice (squares).

$B_0 = m^+(\infty)$, $G_0 = \Delta(\infty)$ and $L = N^{1/2}$. We present the results of the extrapolation for e_0 and m^+ in comparison with the triangular and the kagomé lattice in Table II. The HAFM on the star lattice has lowest GS energy e_0 ; the extrapolated order parameter is finite but very small.

Fig. 5 shows the finite-size behavior of the spin gap of the star lattice in comparison to the kagomé and triangular lattices. We extrapolate a quite big spin gap $\Delta = 0.380$ for the star lattice. For the triangular lattice, the data with $N \leq 36$ seem to suggest a finite spin gap which is, however, spurious. This illustrates that the extrapolation of the spin gap may be most affected by systematic errors.⁷ Nevertheless, the spin gap of the star lattice in Fig. 5 exhibits only comparably small finite-size effects. Hence, the estimation of a non-zero spin gap for the star lattice seems to be reliable. The spin gap extrapolated for the kagomé lattice⁸ is more than six times smaller, but note that the existence of a gap for the kagomé lattice at all is not fully clear, as is also evident from Fig. 5.

V. VARIATIONAL MEAN FIELD APPROACH

We discuss briefly a variational approach which was successfully applied to describe a quantum phase transition between Néel phases and a dimer phase.^{7,26,27} Let us consider a model with different NN bonds J_T and J_D . The GS shall be approximately described by a variational wave function

$$|\Psi\rangle = \prod_{\alpha} \frac{|\phi_+^i(\theta_{\alpha})\rangle|\phi_-^j(\theta_{\alpha})\rangle - t|\phi_-^i(\theta_{\alpha})\rangle|\phi_+^j(\theta_{\alpha})\rangle}{\sqrt{1+t^2}} \quad (3)$$

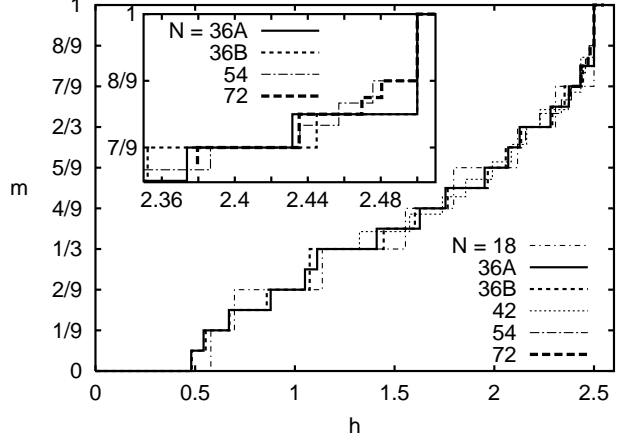


FIG. 6: Magnetization curves for star lattices with $N = 18$, $36A$ and $36B$ (complete) and $N = 42, 54$ and 72 (partial). Inset: High-field part of the magnetization curves for $N = 36A, 36B, 54$ and 72 sites.

where α represents a pair of sites i, j corresponding to a J_D bond. Thus the product in (3) is effectively taken over all J_D bonds of the star lattice. In (3) the vectors $|\phi_{\pm}^i(\theta_{\alpha})\rangle$ are spin up (down) states at site i with a quantization axis corresponding to the classical planar GS considered, i.e. $[\sin(\theta_{\alpha})\hat{S}_i^x + \cos(\theta_{\alpha})\hat{S}_i^z]|\phi_{\pm}^i(\theta_{\alpha})\rangle = \pm\frac{1}{2}|\phi_{\pm}^i(\theta_{\alpha})\rangle$, where the angles θ_{α} correspond to the respective classical $\sqrt{3} \times \sqrt{3}$ or $q=0$ state. $|\Psi\rangle$ depends on the variational parameter t and interpolates between a rotationally invariant dimer product state for $t = 1$ and an uncorrelated planar $\sqrt{3} \times \sqrt{3}$ or $q=0$ state for $t = 0$. Optimizing $\langle\Psi|\hat{H}|\Psi\rangle$ with respect to t we get $E_0^{\text{var}}/\text{bond} = -(J_D^2 + J_D J_T + J_T^2)/12 J_T$. For the sublattice magnetization we obtain

$$M = \langle\Psi|\cos(\theta_{\alpha})\hat{S}_i^z + \sin(\theta_{\alpha})\hat{S}_i^x|\Psi\rangle = \frac{\sqrt{J_T^2 - J_D^2}}{2J_T} \quad (4)$$

for $J_D \leq J_T$. M vanishes with a mean-field critical exponent at the symmetric point $J_D = J_T$. Since such an approach tends to overestimate the region of the semiclassically ordered state,^{26,27} we may interpret the above result as a further indication of a dimerized GS.

VI. MAGNETIZATION PROCESS

Finally, Fig. 6 shows magnetization curves of several finite star lattices, where the magnetization m is defined as $m = 2\langle\hat{S}^z\rangle/N$. Due to computational limitations, only the high-field region can be studied for $N > 36$. For example for $N = 42$, reliable data are available only for $m \geq 1/3$ (and of course $m = 0$, see section IV). Furthermore, the lowest parts of the curves for $N = 54$ ($17/27 \leq m < 19/27$) and $N = 72$ ($3/4 \leq m < 5/6$) are based on assumptions concerning the symmetry of the GS.

First, one observes a pronounced zero-field plateau in Fig. 6 corresponding to the spin gap discussed in section IV. Candidates for further plateaux emerge e.g. at $m = 1/3, 7/9$ and $8/9$. The finite-size effects at the boundaries of these candidate plateaux are comparably weak for $m = 7/9$ (see inset of Fig. 6) such that the numerical evidence in favor of a plateau with $m \neq 0$ is strongest in this case.

The presence of a plateau at $m = 1/3$ is also plausible since the star lattice consists of triangles. More precisely, Ising-like anisotropies can be argued to give rise to a plateau at $m = 1/3$ due to up-up-down configurations on the triangles. The number $\mathcal{N}_{\text{conf.}}$ of such Ising configurations can be determined by explicit enumeration, yielding e.g. $\mathcal{N}_{\text{conf.}} = 123\,528, 3\,508\,392$, and $531\,606\,684$ for the $N = 42, 54$, and 72 lattices, respectively. This number grows asymptotically approximately as $\mathcal{N}_{\text{conf.}} \propto (1.322\ldots)^N$. The number of Ising configurations is much bigger than the corresponding number on the kagomé lattice at $m = 1/3$ (see Ref. 28 and references therein), indicating that the tendency towards a disordered GS at $m = 1/3$ may be stronger on the star lattice than on the kagomé lattice.

Just below saturation, we see a jump in the magnetization curve (see inset of Fig. 6). Indeed, the presence of this jump follows from a general construction of independent localized magnons for strongly frustrated lattices,^{7,29} which in the case of the star lattice live on the dodecagons. The expected height $\delta m = 1/9$ of the jump for sufficiently large N is confirmed for $N = 54$ and 72 (see inset of Fig. 6). Note that the existence of localized magnon states also leads to a finite residual $T = 0$ entropy at the saturation field $h = 5J/2$ ^{7,30} and may favor a tendency towards a spin-Peierls deformation.³¹ On general grounds one expects a plateau just below the jump, i.e. at the candidate value $m = 8/9$ mentioned before,⁷ although the available data do not allow unambiguous confirmation of this plateau.

VII. DISCUSSION AND CONCLUSION

Similar as for the kagomé lattice the results reported in this paper yield indications for a quantum paramagnetic GS for the star lattice, too. Whereas this statement is well-known for the kagomé lattice, the star lattice represents a new example for a quantum HAFM on a uniform 2D lattice without semi-classical GS ordering. However, we emphasize that despite the fact that on the classical and semi-classical level (LSWT) we have very similar physics as for the kagomé lattice (i.e. one zero mode, the classical GS degeneracy is not lifted) the quantum paramagnetic GS for the star lattice is of different nature

than that for the kagomé lattice. The quantum GS for the star lattice is characterized by extremely strong NN correlation on the dimer bonds (more than 60% larger than the NN correlation of the honeycomb lattice having the same coordination number $z = 3$) and a weak NN correlation on the triangular bonds (only about 30% of the NN dimer correlation and significantly less than the triangular NN correlation of the kagomé and the triangular lattices). The singlet-triplet spin gap is particularly large (about six times larger than that for the kagomé lattice). Although the classical GS exhibits a huge non-trivial degeneracy remarkably one does not find low-lying singlets within this large spin gap, rather the first singlet excitation is well above the lowest triplet state. The low-lying spectrum as a whole resembles the spectrum of weakly coupled dimers.⁶ All these features support the conclusion that the quantum GS of the HAFM on the star lattice is dominated by local singlet pairing. This dimerized GS represents a so-called *explicit valence-bond crystal state*,⁸ which respects the lattice symmetry.

Although we could expect a gapped quantum paramagnetic explicit valence-bond crystal GS for the star lattice in case of strong dimer bonds $J_D \gg J_T$, this should be contrasted with other models where an explicit valence-bond crystal GS arises in the limit of strong dimer bonds. For example, in the simple $s = 1/2$ Heisenberg bilayer model, the picture of weakly coupled dimers is qualitatively correct only for an interlayer exchange coupling J_{\perp} significantly larger than the intralayer coupling J ($J_{\perp} \gtrsim 2.5J$, see Refs. 26,32 and references therein). Because the bilayer Heisenberg model is not frustrated, the classical GS does not exhibit any non-trivial degeneracy and the GS remains the semi-classical Néel state for $J_{\perp} \approx J$ and all values of s .³² By contrast, the quantum paramagnetic GS appears in the $s = 1/2$ star lattice even in the *uniform* case $J_D = J_T$. This difference can be attributed to the strong frustration present in the star lattice.

The magnetization curve of the $s = 1/2$ HAFM on the star lattice shows a jump just below saturation and several candidates for plateaux e.g. at $m = 1/3, 7/9$ and $8/9$ as some typical features of strongly frustrated quantum spin lattices. Furthermore, low-energy excitations present for certain magnetic fields promise large magnetocaloric effects.³⁰

Acknowledgments

We are indebted to H.-U. Everts for valuable discussions. This work was partly supported by the DFG (project Ri615/12-1).

¹ S. Taniguchi, T. Nishikawa, Y. Yasui, Y. Kobayashi, M. Sato, T. Nishioka, M. Kontani, K. Sano, J. Phys. Soc.

Jpn. **64**, 2758 (1995).

² H. Kageyama, K. Yoshimura, R. Stern, N.V. Mushnikov,

- K. Onizuka, M. Kato, K. Kosuge, C.P. Slichter, T. Goto, Y. Ueda, Phys. Rev. Lett. **82**, 3168 (1999).
- ³ R. Coldea, D.A. Tennant, Z. Tyliczynski, Phys. Rev. B **68**, 134424 (2003).
- ⁴ H. Tanaka, T. Ono, H.A. Katori, H. Mitamura, F. Ishikawa, T. Goto, Progr. Theor. Phys. Suppl. **145**, 101 (2002).
- ⁵ B. Grünbaum, G.C. Shephard, *Tilings and Patterns*, W.H. Freeman and Company, New York (1987).
- ⁶ J. Schulenburg, PhD thesis, University of Magdeburg (2002) [<http://www-e.uni-magdeburg.de/jschulen/diss.html>].
- ⁷ J. Richter, J. Schulenburg, A. Honecker, Lect. Notes Phys. **645**, 85-153 (2004).
- ⁸ G. Misguich, C. Lhuillier, *Two-dimensional quantum antiferromagnets*, \protect\vrule{width0pt}{\protect\href{http://arXiv.org/abs/cond-mat/0310059}{arXiv.org/abs/cond-mat/0310059}} (2003).
- ⁹ C. Lhuillier, P. Sindzingre, J.-B. Fouet, Can. J. Phys. **79**, 1525 (2001).
- ¹⁰ R. Moessner, Can. J. Phys. **79**, 1283 (2001).
- ¹¹ D. Schmalfuß, P. Tomczak, J. Schulenburg, J. Richter, Phys. Rev. B **65**, 224405 (2002).
- ¹² P. Tomczak, J. Richter, Phys. Rev. B **59**, 107 (1999).
- ¹³ P. Tomczak, J. Schulenburg, J. Richter, A.R. Ferchmin, J. Phys.: Condens. Matter **13**, 3851 (2001).
- ¹⁴ B. Normand, K. Penc, M. Albrecht, F. Mila, Phys. Rev. B **56**, R5736 (1997).
- ¹⁵ S. Miyahara, M. Troyer, D.C. Johnston, K. Ueda, J. Phys. Soc. Jpn. **67**, 3918 (1998).
- ¹⁶ A.B. Harris, C. Kallin, A.J. Berlinsky, Phys. Rev. B **45**, 2899 (1992).
- ¹⁷ J.T. Chalker, P.C.W. Holdsworth, E.F. Shender, Phys. Rev. Lett. **68**, 855 (1992); E.F. Shender, P.C.W. Holdsworth, In *Fluctuations and Order: a new synthesis*, M.M. Millonas ed., Springer-Verlag (1996).
- ¹⁸ H. Asakawa, M. Suzuki, Physica A **205**, 687 (1994).
- ¹⁹ D.D. Betts, J. Schulenburg, G.E. Stewart, J. Richter, J.S. Flynn, J. Phys. A: Math. Gen. **31**, 7685 (1998).
- ²⁰ P.W. Leung, V. Elser, Phys. Rev. B **47**, 5459 (1993).
- ²¹ B. Bernu, P. Lecheminant, C. Lhuillier, L. Pierre, Phys. Rev. B **50**, 10048 (1994).
- ²² P. Lecheminant, B. Bernu, C. Lhuillier, L. Pierre, P. Sindzingre, Phys. Rev. B **56**, 2521 (1997).
- ²³ Ch. Waldtmann, H.-U. Everts, B. Bernu, C. Lhuillier, P. Sindzingre, P. Lecheminant, L. Pierre, Eur. Phys. J. B **2**, 501 (1998).
- ²⁴ H. Neuberger, T. Ziman, Phys. Rev. B **39**, 2608 (1989).
- ²⁵ P. Hasenfratz, F. Niedermayer, Z. Phys. B **92**, 91 (1993).
- ²⁶ C. Gros, W. Wenzel, J. Richter, Europhys. Lett. **32**, 747 (1995).
- ²⁷ S.E. Krüger, J. Richter, J. Schulenburg, D.J.J. Farnell, \protect\vrule{width0pt}{\protect\href{http://arXiv.org/abs/cond-mat/0310059}{arXiv.org/abs/cond-mat/0310059}} (2003).
- ²⁸ D.C. Cabra, M.D. Grynberg, P.C.W. Holdsworth, A. Honecker, P. Pujol, J. Richter, D. Schmalfuß, J. Schulenburg, \protect\vrule{width0pt}{\protect\href{http://arXiv.org/abs/cond-mat/0402009}{arXiv.org/abs/cond-mat/0402009}} (2004).
- ²⁹ J. Schulenburg, A. Honecker, J. Schnack, J. Richter, H.-J. Schmidt, Phys. Rev. Lett. **88**, 167207 (2002); J. Richter, J. Schulenburg, A. Honecker, J. Schnack, H.-J. Schmidt, J. Phys.: Condens. Matter **16**, S779 (2004).
- ³⁰ O. Derzhko, J. Richter, Phys. Rev. B **70**, 104415 (2004); M.E. Zhitomirsky, A. Honecker, J. Stat. Mech.: Theor. Exp. P07012 (2004); M.E. Zhitomirsky, H. Tsunetsugu, Phys. Rev. B **70**, 100403(R) (2004).
- ³¹ J. Richter, O. Derzhko, J. Schulenburg, Phys. Rev. Lett. **93**, 107206 (2004).
- ³² M.P. Gelfand, Zheng Weihong, C.J. Hamer, J. Oitmaa, Phys. Rev. B **57**, 392 (1998); M. Troyer, S. Sachdev, Phys. Rev. Lett. **81**, 5418 (1998).